

# Gold nanoparticles supported on ceria-modified mesoporous–macroporous binary metal oxides as highly active catalysts for low-temperature water–gas shift reaction

V. Idakiev · T. Tabakova · K. Tenchev · Z. Y. Yuan ·  
T. Z. Ren · A. Vantomme · B. L. Su

Received: 28 November 2008 / Accepted: 12 May 2009 / Published online: 2 June 2009  
© Springer Science+Business Media, LLC 2009

**Abstract** New gold catalytic system prepared on ceria-modified meso-/macroporous binary metal oxide support ( $\text{CeO}_2/\text{TiO}_2\text{-ZrO}_2$ ) and used as water–gas shift reaction (WGS) catalyst is reported. The support was prepared through the surfactant templating technique combining with the use of mixed alkoxide solutions. Ceria-modifying additive and gold were deposited consecutively on the meso-/macroporous  $\text{TiO}_2\text{-ZrO}_2$  by deposition-precipitation method. The samples were characterized by powder X-ray diffraction, scanning and transmission electron microscopy,  $\text{N}_2$  adsorption analysis, and temperature-programmed reduction. The catalytic activity of the new gold-based catalysts was evaluated in WGS and it was compared with that of gold catalysts supported on simple and binary mesoporous oxides ( $\text{TiO}_2$ ,  $\text{ZrO}_2$ , and  $\text{TiO}_2\text{-ZrO}_2$ ) and ceria-modified mesoporous titania support ( $\text{CeO}_2/\text{mTiO}_2$ ). A high degree of synergistic interaction between ceria and support and a positive modification of structural and catalytic properties

have been achieved. The new gold catalytic system is found to be a promising catalyst for practical WGS application.

## Introduction

The removal of carbon monoxide by water–gas shift reaction (WGS) is an important step in a number of chemical processes for  $\text{H}_2$  production [1, 2]. Based on work to date, it is considered likely that supported gold nanoparticles could form the basis for catalytic systems with potential commercial application in the generation and purification of hydrogen streams for fuel cells. The type of the support is found to be the critical parameter, which determines the catalytic activity and stability. The mesoporous materials with different compositions, new pore systems, and novel properties have attracted considerable attention because of their remarkably large surface areas and narrow pore size distributions, which make them ideal candidates for catalysts [3, 4]. The structure of mesoporous oxide supports facilitates the formation of well-dispersed and stable gold particles on the surface upon calcination and reduction and thus strongly improves the catalytic performances. It was suggested a good possibility to apply these materials for the first time as supports for gold catalysts [5]. Mesoporous titania, zirconia, and ceria due to their attracting mesostructural features have been found to be promising supports for gold-based catalysts used in WGS [6–8]. The catalytic activity and especially the stability of gold catalysts strongly depend on both the state and structure of the support and the specific interaction between gold and support. Recently, Au-ceria catalysts have also been reported as exhibiting very interesting properties for the low-temperature WGS [9–17]. Ceria is known to affect the dispersion of supported metals. The

---

V. Idakiev (✉) · T. Tabakova · K. Tenchev  
Institute of Catalysis, Bulgarian Academy of Sciences,  
1113 Sofia, Bulgaria  
e-mail: idakiev@ic.bas.bg

Z. Y. Yuan  
Institute of New Catalytic Materials Science,  
College of Chemistry, Nankai University,  
Tianjin 300071, People's Republic of China

T. Z. Ren  
School of Chemical Engineering, Hebei University  
of Technology, Tianjin 300130, People's Republic of China

A. Vantomme · B. L. Su (✉)  
Laboratory of Inorganic Materials Chemistry,  
The University of Namur (FUNDP), 5000 Namur, Belgium  
e-mail: bao-lian.su@fundp.ac.be

promotion by noble or transition metal enhances the ceria reducibility and facilitates the generation of very active centers at the interface between metal and support. The availability of nanosized gold particles on the surface in close contact with ceria plays a decisive role for high activity and stability of these catalysts [16, 18].

Hierarchical materials containing both interconnected macroporous and mesoporous structures have enhanced properties compared with single-sized pore materials due to increased mass transport through the material and maintenance of a specific surface area on the level of fine pore systems [19]. The structural and textural properties of the meso-/macrostructured single metal oxides could be improved by the introduction of secondary oxide to form the binary metal oxide composite materials [20]. The synthesized binary mixed oxides have a homogeneous distribution of the components and higher surface areas than the single metal oxides. The thermal stability of the binary oxide compositions could also be enhanced significantly. These meso-/macrostructured binary oxide compositions should be beneficial for the use as advanced functional materials, especially in the catalysis applications. Meso-/macroporous titanium and zirconium phosphates [21–23] have been found to possess a large quantity of acid sites, suggesting the possibility of surface functionalization for practical applications in catalysis. The meso-/macroporous  $\text{ZrO}_2$ ,  $\text{TiO}_2$ , and  $\text{ZrO}_2\text{--TiO}_2$  were used as supports for Pd catalysts, and tested for total oxidation of volatile organic compounds (VOCs) [24]. The  $\text{Ce}_{0.8}\text{Zr}_{0.2}\text{O}_2$  material was used as a catalyst support of high-efficiency CO oxidation catalyst ( $\text{CuO}/\text{Ce}_{0.8}\text{Zr}_{0.2}\text{O}_2$ ) [25].

The aim of this research work is to prepare new gold-based catalysts supported on hierarchically meso-/macroporous nanostructured oxide materials and study their catalytic behavior in the WGS. The supports of these new gold catalytic systems concern a binary oxide composition, including titania and zirconia with a meso-/macroporous structure and ceria-modifying additive. In this study, we reveal the relationship between textural and structural characteristics of prepared meso-/macroporous binary metal oxides, their modification by ceria, and WGS activity. We discuss the catalytic behavior of these catalysts based on their full characterization to unravel the role of ceria-modifying additive and possible interaction between gold nanoparticles and ceria-meso-/macroporous support.

## Experimental

### Synthesis of meso-/macroporous mixed oxide support

The meso-/macroporous mixed oxide ( $\text{TiO}_2\text{--ZrO}_2$ ) was prepared as follows: a micellar solution (15 wt%) of

decaoxyethylenecetyl ether ( $\text{C}_{16}(\text{EO})_{10}$ ) was prepared by dissolving the surfactant at room temperature in an aqueous solution for 3 h. A mixture containing 0.05 mol of zirconium *n*-propoxide ( $[\text{Zr}(\text{OC}_3\text{H}_7)_4]$ , 70 wt% in 1-propanol) and 0.05 mol of titanium propoxide was added drop wise to the above medium, followed by further stirring for 3 h at room temperature. The obtained mixture was then transferred into a Teflon-lined autoclave and heated under static conditions at 60 °C for 48 h. The product was filtered and washed by Soxhlet extraction over ethanol for 36 h to remove the surfactant species. The molar ratio of the meso-/macroporous mixed oxide is:  $\text{Ti}:\text{Zr} = 5:5$ . The sample was labeled as TiZr.

### Preparation of ceria-modified meso-/macroporous mixed oxide

Ceria was loaded on meso-/macroporous mixed oxide ( $\text{TiO}_2\text{--ZrO}_2$ ) by deposition-precipitation (DP) method. Before deposition, the meso-/macroporous material was suspended in water by ultrasound technique. Ceria was deposited by precipitation of  $\text{Ce}(\text{NO}_3)_3 \cdot 6\text{H}_2\text{O}$  with  $\text{Na}_2\text{CO}_3$  at 60 °C and pH 9.0. The precipitate was aged in a course of 1 h at the same temperature, filtered, and washed carefully until absence of  $\text{NO}_3^-$  ions. The sample was dried under vacuum at 80 °C and calcined in air at 400 °C for 2 h. Ceria-modifying additive is 20 wt%. The sample was labeled as CeTiZr.

### Preparation of gold-containing catalysts

Gold was loaded on prepared supports (TiZr and CeTiZr) by DP method. The gold hydroxide was supported on supports preliminarily suspended in water via the chemical reaction between  $\text{HAuCl}_4 \cdot 3\text{H}_2\text{O}$  and  $\text{Na}_2\text{CO}_3$  in aqueous solution. The precipitates were aged for 1 h at 60 °C, filtered, and washed carefully until  $\text{Cl}^-$  ions are completely removed. The samples were dried under vacuum at 80 °C and calcined in air at 400 °C for 2 h. The catalysts were denoted as Au/TiZr and Au/CeTiZr for the samples prepared on meso-/macroporous mixed oxide (TiZr) and on ceria-modified support (CeTiZr), respectively. The gold loading for the catalysts is 3 wt%.

All DP procedures were carried out in “Contalab” laboratory reactor (Conraves AG, Switzerland) under complete control of all parameters: temperature, pH, stirrer speed, and reactant feed flow rates. All chemicals used were of analytical grade.

### Sample characterization

X-ray powder diffraction (XRD) patterns were obtained on a Philips PW 170 diffractometer using  $\text{Cu K}\alpha$  (1.54178 Å)

radiation and the measurements were carried out in the  $2\theta$  angle range of  $10\text{--}60^\circ$ .  $\text{N}_2$  adsorption–desorption isotherms were determined on a Micromeritics TRISTAR 3000 system at liquid nitrogen temperature ( $-196^\circ\text{C}$ ). The surface area was obtained by the Brunauer–Emmett–Teller (BET) method, and the pore size distribution was calculated from the adsorption branch of the isotherm by the Barret–Joyner–Halenda (BJH) model. Scanning electron microscopy (SEM) and transmission electron microscopy (TEM) were carried out with a Philips XL-20 at 15 keV and a Philips TECNAI-10 at 100 kV, respectively. The specimens for TEM observation were prepared by epoxy resin-embedded microsectioning and mounting on a copper grid. Temperature-programmed reduction (TPR) of the samples was carried out in the measurement cell of a differential scanning calorimeter (DSC) model DSC-111 (SETARAM) directly connected to a gas chromatograph (GC). A quartz reactor was loaded with 0.17 g of calcined samples. The measurements were performed in the range of  $20\text{--}700^\circ\text{C}$  at  $15^\circ\text{C}/\text{min}$  heating rate in flow of 10%  $\text{H}_2/\text{Ar}$ , the total flow rate being 25 mL/min. A cooling trap between DSC and GC removed the water obtained during the reduction. The samples were calcined at  $400^\circ\text{C}$  in synthetic air (20%  $\text{O}_2$  in Ar) for 30 min before the TPR measurements. The gold content in catalysts was analyzed by atomic adsorption method.

#### Catalytic activity measurement

Catalytic activity tests were performed in a fixed-bed flow reactor at atmospheric pressure and temperature range from 140 to  $300^\circ\text{C}$ . Prior to all catalytic tests, the samples were heated in a flowing 20 vol.%  $\text{O}_2/\text{Ar}$  mixture at  $400^\circ\text{C}$  for 30 min as a standard pretreatment to yield clean surfaces. The following conditions were applied: catalyst bed volume  $0.5\text{ cm}^3$ , space velocity  $4000\text{ h}^{-1}$ , partial pressure of water vapor 31.1 kPa, and the reactant gas mixture contained 4.492 vol.% CO in argon. The CO and  $\text{CO}_2$  content was analyzed on “URAS-3G” and “URAS-2T” (Hartmann & Braun AG) gas analyzers and the catalytic activity was expressed by degree of CO conversion.

## Results and discussion

#### Structural and textural characterization

##### XRD, SEM, and TEM analysis

Low-angle XRD patterns of TiZr sample gave a broad peak between  $1^\circ$  and  $3^\circ$  of  $2\theta$ , characteristic of a disordered mesostructure with no discernible long-range order in the mesopore arrangement [26]. The disordered mesostructure

is consistent with TEM observations (Fig. 2b). The wide-angle XRD patterns of the supports (TiZr and CeTiZr) and gold-based catalyst (Au/CeTiZr) are shown in Fig. 1. No distinct diffraction lines of titania and zirconia could be detected by XRD in the TiZr sample, indicating a homogeneous mixing of the Ti and Zr oxides and their amorphous character. This suggests that the segregation did not occur, and meso-/macrostructured TiZr were formed with (Ti,Zr)- $\text{O}_2$  species, a real solid solution of  $\text{TiO}_2$  and  $\text{ZrO}_2$ , rather than discrete  $\text{TiO}_2$  and  $\text{ZrO}_2$  nanocrystallites. There are no significant differences in the XRD patterns after deposition of ceria additive. The results revealed the beneficial role of ceria additive in decreasing the degree of crystallinity of TiZr and decreasing its particle size. No significant differences after deposition of gold can be detected, which may be due to the high dispersion of the gold nanoparticles.

The meso-/macrostructures are retained after calcination at  $400^\circ\text{C}$ , as revealed by SEM and TEM images. SEM images revealed that the synthesized TiZr is composed of particles with macroporous structures (Fig. 2a). A lot of particles are found to contain a macroporous array having diameters of 0.6–3 nm. A regular array of the macropores can clearly be seen. Moreover, the macropores are usually of one-dimensional orientation, parallel to each other and orthogonal to one side of the monolithic particles. These well-oriented macrochannels extend through almost the whole particle. The wall thickness between the macropores with circular openings is around 0.3–3  $\mu\text{m}$ . High-magnification TEM images of the cross-sectional TiZr specimen also reveal that the macroporous framework is composed of nanoparticles with accessible and interconnected mesopores of a disordered wormhole-like array (Fig. 2b).

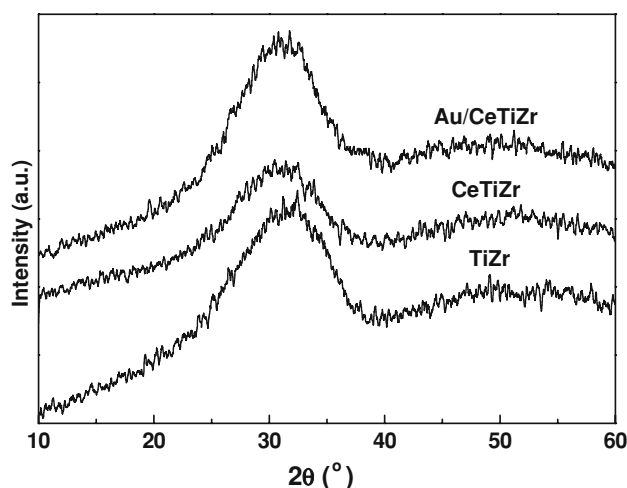


**Fig. 1** X-ray diffraction patterns of the calcined supports (TiZr and CeTiZr) and gold-based catalyst (Au/CeTiZr)

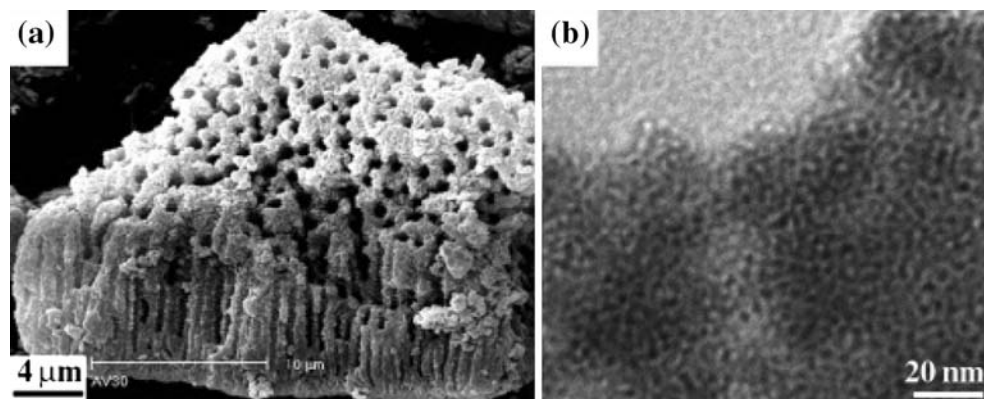


**Fig. 2** **a** SEM image of the meso-/macroporous TiZr composite. **b** TEM image of the macropore walls of **(a)**

### Nitrogen adsorption analysis

The  $N_2$  adsorption–desorption isotherms (a) and the corresponding BJH pore size distribution curves (b) of the supports (TiZr and CeTiZr) and the gold-based catalysts (Au/TiZr and Au/CeTiZr) are shown in Fig. 3. The increase in

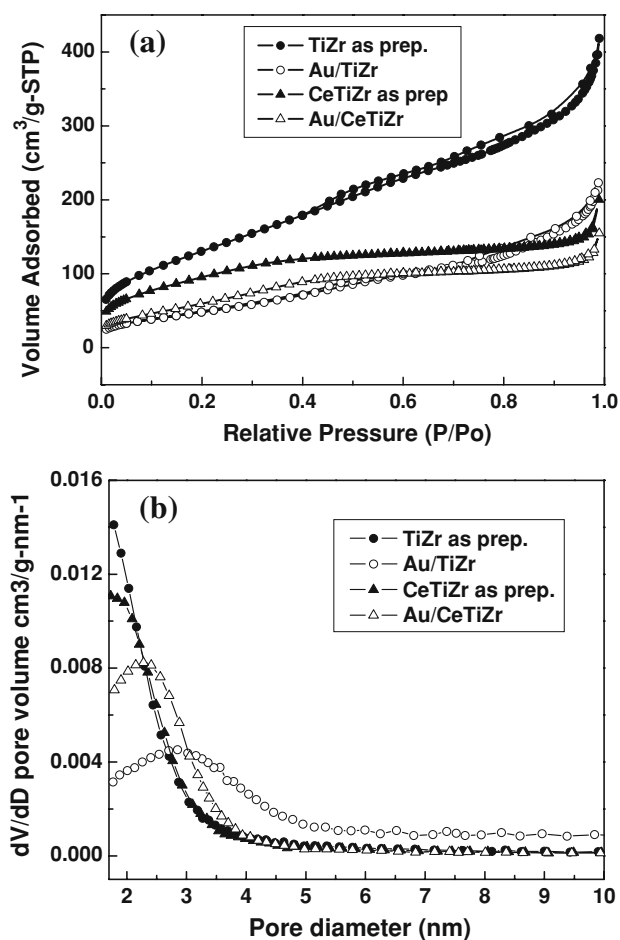


**Fig. 3** Nitrogen adsorption isotherms **(a)** and the corresponding BJH pore size distribution curves **(b)** of the supports (TiZr and CeTiZr) and the gold-based catalysts (Au/TiZr and Au/CeTiZr)

adsorbed volume at high relative pressure is a direct indication of the presence of the secondary large pores. In general, all samples based on TiZr support exhibit quite narrow pore size distribution peaks, indicative of the homogeneity of the mesoporosity of our materials, with higher surface areas and larger pore volumes. The textural properties of the obtained samples are listed in Table 1. The BET surface areas of the calcined supports are larger than those of the calcined gold-based catalysts. The decreasing of the value is insignificant, about 5–10%. The surface area of the calcined TiZr remains higher than  $200 \text{ m}^2/\text{g}$ . The pure mesoporous zirconia and titania have surface areas of only 140 and  $125 \text{ m}^2/\text{g}$ , respectively, after calcination, indicating the higher thermal stability of the TiZr meso-/macroporous materials [6, 7]. After ceria deposition on TiZr meso-/macroporous support, the pore volume significantly decreases (Table 1) due to, most probably, some insertion of the ceria additive into the pores. The binary oxides were either bi-crystalline with low crystallinity, noncrystalline, or amorphous. This suggests that the mixing of secondary oxides could inhibit the crystallite growth not only during the synthesis but also upon heat treatment and make the materials more stable against the phase transformations (for example, anatase-to-rutile, amorphous-to-tetrahedral  $ZrO_2$ ) upon calcination. Thus, the amorphous structure is observed in the calcined composites instead of crystalline phases. Consequently, thermally stable binary oxides could be obtained with higher surface areas than the single metal oxides.

### TPR measurements

Figure 4 illustrates the TPR profiles of the supports (TiZr and CeTiZr) and their corresponding gold catalysts (Au/TiZr and Au/CeTiZr). In the profile of meso-/macroporous support (TiZr), only a peak at above  $580^\circ\text{C}$  due to the titania reduction is observed. The modification with ceria causes strong effect on the reducibility of meso-/macroporous support (CeTiZr) and the peak is shifted to  $365^\circ\text{C}$ .

**Table 1** Textural properties of the supports and gold-based catalysts, the gold content, and average size of gold particles in the catalysts

Sample	Calcination temperature (°C)	Specific surface area (m <sup>2</sup> /g) <sup>a</sup>	Pore diameter (nm) <sup>b</sup>	Pore volume (cm <sup>3</sup> /g) <sup>c</sup>	Au content (wt%) <sup>d</sup>	Au particle size (nm) <sup>e</sup>
TiZr	80	720	2.2	0.92	–	–
	500	205	3.1	0.39	–	–
Au/TiZr	400	183	2.9	0.35	2.47	<4.0
CeTiZr	80	356	1.7	0.31	–	–
	400	245	2.0	0.20	–	–
Au/CeTiZr	400	233	2.3	0.24	2.64	<4.0

<sup>a</sup> Total surface area estimated by BET method

<sup>b</sup> Pore diameter corresponding to the maximum on the pore size distribution curve

<sup>c</sup> Total pore volume at  $p/p_0 = 0.99$

<sup>d</sup> Analyzed by atomic adsorption method

<sup>e</sup> Determined by XRD method

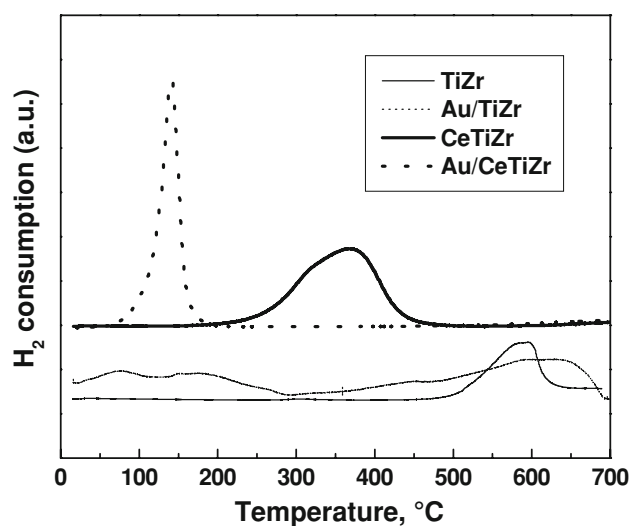


**Fig. 4** TPR profiles of the supports (TiZr and CeTiZr) and gold-based catalysts (Au/TiZr and Au/CeTiZr) calcined at 400 °C

This enhanced reducibility could be related to the synergistic interaction between ceria and the meso-/macroporous support (TiZr) in agreement with the results from the other characterization methods used. Clear evidence that gold facilitates the reducibility of the CeTiZr support is found by H<sub>2</sub>-TPR. An intense and sharp low-temperature (LT) peak with  $T_{\max} = 140$  °C is observed in the TPR profile of Au/CeTiZr. The LT peak can be assigned to the reduction of oxygen species on the nanosized gold particles and to the almost fully reduction of the support. In the curve of gold-supported meso-/macroporous support (TiZr), besides the high-temperature peak ( $T_{\max} = 620$  °C), two LT peaks ( $T_{\max} = 75$  and  $175$  °C) are registered. Such behavior has already been observed for the Au/mesoporous titania samples [6]. We assign the LT peaks to the reduction of oxygen species on the nanosized gold particles and to the

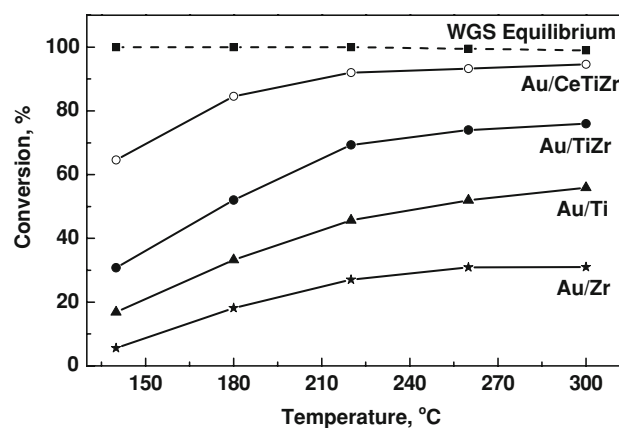


**Fig. 5** WGS activity of the catalyst (Au/CeTiZr) compared with that of gold catalysts supported on pure and binary mesoporous oxides ZrO<sub>2</sub> (Au/Zr, [7]), TiO<sub>2</sub> (Au/Ti, [6]), and TiO<sub>2</sub>/ZrO<sub>2</sub> (Au/TiZr). The equilibrium conversion is shown for comparison

support reduction on the border with gold particles. The HT peak is quite broad and shifted to lower temperatures in comparison with HT one of meso-/macroporous support (TiZr). Comparing with the spectrum of Au/CeTiZr sample, the LT peaks of the Au/TiZr sample are significantly weaker and with lower intensity. The differences in the peak shape and position depending on the nature of the supports are clearly seen.

#### Catalytic activity

The catalytic activity of the gold-based catalysts was evaluated in the WGS in a wide temperature range of 140–300 °C, space velocity 4000 h<sup>-1</sup>, and partial pressure of the water vapor 31.1 kPa. Figure 5 shows the WGS activity of the prepared gold catalysts on Ce-modified TiZr

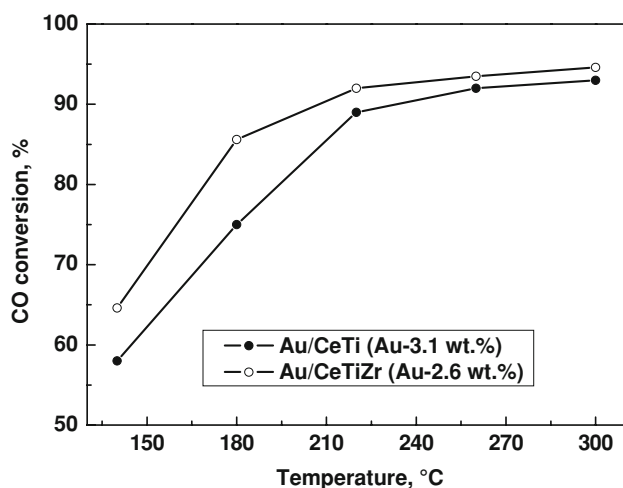


**Fig. 6** WGS activity of the new catalyst (Au/CeTiZr) compared with that of gold catalyst supported on ceria-modified mesoporous titania (Au/CeTi [18])

support (Au/CeTiZr) compared with that of gold catalysts supported on pure and binary mesoporous oxides, ZrO<sub>2</sub> (Au/Zr), TiO<sub>2</sub> (Au/Ti), and TiO<sub>2</sub>/ZrO<sub>2</sub> (Au/TiZr). The activity of the binary metal oxide TiZr and ceria-modified TiZr in this temperature region in WGS is imperceptible. The addition of gold significantly increases the catalytic activity of the samples. The comparison of CO conversion of the gold catalyst (Au/CeTiZr) with the other gold catalysts indicates that the catalyst prepared on the ceria-modified TiZr exhibited superior catalytic activity. A high degree of synergistic interaction between ceria additive and TiZr support was observed. Figure 6 confirms this beneficial effect of ceria modification of binary TiZr support. The WGS activity of the ceria-modified TiZr gold catalyst (Au/CeTiZr) compared with that of the gold catalyst prepared on ceria-modified mesoporous titania is significantly higher. The different catalytic behavior of Au/CeTiZr and Au/CeTi catalysts indicate that the processes occurring on the catalyst surface strongly depend on the nature of the support. Catalytic activity is controlled by the contact structure of Au nanoparticles with the support, the selection of the support materials, and the size of Au particles [27]. The higher activity of the sample Au/CeTiZr could be related to the contact structure of Au nanoparticles with the support. The data in Table 1 and presented in [6, 7] show that the specific surface area of the catalysts has the following order: Au/CeTiZr > Au/TiZr > Au/Ti > Au/Zr. The same catalytic behavior was observed by us in activity of the catalysts. It is reasonable to suppose that the number of active sites located at the Au/support interface on the surface of Au/CeTiZr sample is larger. Figure 5 also shows high degree of synergistic interaction between titania and zirconia. The gold catalyst prepared on binary meso-/macroporous support (TiZr) possesses significantly higher catalytic activity in

comparison with that of gold catalysts supported on pure mesoporous titania and zirconia. The observed WGS activity of the catalytic samples correlates well with the aforementioned H<sub>2</sub>-TPR result. The ceria additive interacts with the meso-/macroporous support (TiZr) and induces strong effect on the reducibility of the support, and the gold loading significantly promotes the reducibility of ceria-modified meso-/macroporous binary metal oxides CeTiZr. The presence of gold and ceria species makes easy the formation of oxygen defects at the surface, which strongly improves the catalytic performance.

## Summary

New gold catalyst has been prepared on ceria-modified meso-/macroporous binary metal oxide support (CeO<sub>2</sub>/TiO<sub>2</sub>-ZrO<sub>2</sub>) and evaluated in WGS reaction. The support was synthesized through the surfactant templating technique combining with the use of mixed alkoxide solutions. Ceria-modifying additive and gold were deposited consecutively on support by DP method. No crystalline phase was observed by XRD in the prepared supports and catalysts, indicating a homogeneous mixing of the components. The results revealed the beneficial role of ceria additive in decreasing the degree of crystallinity of TiZr and decreasing its particle size. TEM images reveal that the macroporous framework is composed of nanoparticles with accessible and interconnected mesopores of a disordered wormhole-like array. All samples exhibit quite narrow pore size distribution peaks, indicative of the homogeneity of the mesoporosity of our materials, with high surface areas and large pore volumes. The ceria additive induces strong effect on the reducibility of the support, as well as the gold loading significantly promotes the reducibility of ceria-modified support (CeTiZr). The presence of gold and ceria species makes easy the formation of oxygen defects at the surface, which strongly improves the catalytic performance. A high degree of synergistic interaction between ceria and support and a positive modification of structural and catalytic properties has been achieved. High catalytic efficiency can be explained by the high structural homogeneity, availability of more oxygen vacancies, and an enlarged surface area. The nature of the support is of crucial importance in obtaining highly dispersed gold particle and catalysts with good performance. The new gold catalytic system is found to be a promising catalyst for practical WGS application.

**Acknowledgements** The Joint Research Project between the Commissariat general des relations internationales (CGRI), Belgium and Bulgarian Academy of Sciences (BAS), the Chinese-Bulgarian Scientific and Technological Cooperation Project (2K-11-01/2006), the Belgian Federal Government (Belspo PAI-IAP project, INANOMAT,

P6/17), and the National Basic Research Program of China (No. 2009CB623502) supported this work.

## References

1. Twigg M (ed) (1996) Catalyst handbook. Manson, London
2. Trimm DL (2005) Appl Catal A 296:1
3. Trong On D, Displantier-Giscard D, Dalumash C, Kaliagunine S (2001) Appl Catal A 222:299
4. Trong On D, Displantier-Giscard D, Dalumash C, Kaliagunine S (2003) Appl Catal A 253:545
5. Idakiev V, Ilieva L, Andreeva D, Blin JL, Gigot L, Su BL (2003) Appl Catal A 243:25
6. Idakiev V, Tabakova T, Yuan ZY, Su BL (2004) Appl Catal A 270:135
7. Idakiev V, Tabakova T, Naydenov A, Yuan ZY, Su BL (2006) Appl Catal B 63:178
8. Yuan ZY, Idakiev V, Vantomme A, Tabakova T, Ren TZ, Su BL (2008) Catal Today 131:203
9. Trovarelli A (1996) Catal Rev Sci Eng 38:439
10. Andreeva D, Idakiev V, Tabakova T, Ilieva L, Falaras P, Bourlinos A, Travlos A (2002) Catal Today 72:51
11. Fu Q, Weber A, Flytzani-Stephanopoulos M (2001) Catal Lett 77:87
12. Luengaruemitchai A, Osuwan S, Gulabi E (2003) Catal Commun 4:215
13. Goerke O, Pfeifer P, Schubert K (2004) Appl Catal A 263:11
14. Kim CH, Thompson LT (2005) J Catal 230:66
15. Sakurai H, Akita T, Tsubota S, Kiuchi M, Haruta M (2005) Appl Catal A 291:179
16. Tabakova T, Boccuzzi F, Manzoli M, Sobczak JW, Idakiev V, Andreeva D (2004) Appl Catal B 49:73
17. Fu Q, Deng W, Saltsburg H, Flytzani-Stephanopoulos M (2005) Appl Catal B 56:57
18. Idakiev V, Tabakova T, Tenchev K, Yuan ZY, Ren TZ, Su BL (2007) Catal Today 128:223
19. Yuan ZY, Su BL (2006) J Mater Chem 16:663
20. Yuan ZY, Ren TZ, Vantomme A, Su BL (2004) Chem Mater 16:5096
21. Ren TZ, Yuan ZY, Su BL (2004) Chem Commun 23:2730
22. Ren TZ, Yuan ZY, Azioune A, Su BL (2006) Langmuir 22:3886
23. Yuan ZY, Ren TZ, Azioune A, Pireaux JJ, Su BL (2005) Catal Today 105:647
24. Tidahy NL, Siffert S, Lamonier JF, Zhilinskaya EA, Aboukaïs A, Yuan ZY, Vantomme A, Su BL, Canet X, Deweyreld G, Frere M, N'Guyen TB, Gireaudon JM, Leclercq G (2006) Appl Catal A 310:61
25. Cao JL, Wang Y, Zhang TY, Wu SH, Yuan ZY (2008) Appl Catal B 78:120
26. Bagshaw SA, Pinnavaia TJ (1996) Angew Chem Int Ed Engl 35:1102
27. Haruta M (2002) Catech 6:102